HHS Public Access

Author manuscript

J Mol Biol. Author manuscript; available in PMC 2019 September 14.

Published in final edited form as:

J Mol Biol. 2018 September 14; 430(18 Pt B): 3323–3336. doi:10.1016/j.jmb.2018.06.025.

Species-specific Functions of Twinfilin in Actin Filament Depolymerization

Denise M. Hilton[1], **Rey M. Aguilar**[1], **Adam B. Johnston**[1], and **Bruce L. Goode**[1,*]

[1]Department of Biology, Rosenstiel Basic Medical Science Research Center, Brandeis University, Waltham, MA, 02454, USA

Abstract

Twinfilin is a highly conserved member of the actin depolymerization factor homology (ADF-H) protein superfamily, which also includes ADF/Cofilin, Abp1/Drebrin, GMF, and Coactosin. Twinfilin has a unique molecular architecture consisting of two ADF-H domains joined by a linker and followed by a C-terminal tail. Yeast Twinfilin, in conjunction with yeast cyclase-associated protein (Srv2/CAP), increases the rate of depolymerization at both the barbed and pointed ends of actin filaments. However, it has remained unclear whether these activities extend to Twinfilin homologs in other species. To address this, we purified the three mouse Twinfilin isoforms (mTwf1, mTwf2a, mTwf2b) and mouse CAP1, and used TIRF microscopy assays to study their effects on filament disassembly. Our results show that all three mouse Twinfilin isoforms accelerate barbed end depolymerization similar to yeast Twinfilin, suggesting that this activity is evolutionarily conserved. In striking contrast, mouse Twinfilin isoforms and CAP1 failed to induce rapid pointed end depolymerization. Using chimeras, we show that the yeast-specific pointed end depolymerization activity is specified by the C-terminal ADF-H domain of yeast Twinfilin. Additionally, Tropomyosin decoration of filaments failed to impede depolymerization by yeast and mouse Twinfilin and Srv2/CAP, but inhibited Cofilin severing. Together, our results indicate that Twinfilin has conserved functions in regulating barbed end dynamics, although its ability to drive rapid pointed end depolymerization appears to be species-specific. We discuss the implications of this work, including that pointed end depolymerization may be catalyzed by different ADF-H family members in different species.

Graphical Abstract

[*]To whom correspondence should be addressed: Bruce L. Goode, Rosenstiel Basic Medical Science Research Center, Brandeis University, 415 South St., Waltham MA, 02454, Tel. 781 - 736-2464, Fax 781-736-2405, goode@brandeis.edu.

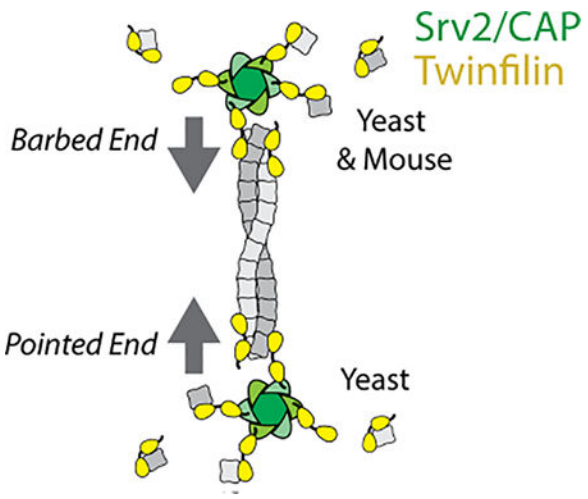

Keywords

Actin; Cofilin; ADF; ADF-H domain; depolymerization

INTRODUCTION

Cellular actin networks vary greatly in their size, filamentous architecture, decoration by different actin-binding proteins, and turnover dynamics. The lifetimes of actin subunits in these structures range from 10–20 seconds (e.g., leading edge and sites of endocytosis), to minutes, hours, or even days (e.g., stereocilia and muscle fibers). Further, the turnover rate of subunits within a network can change dramatically at specific stages of the network life cycle or function, e.g., upon lamellipodial network transitions from a state of net assembly during protrusion to a state of net disassembly during retraction. Thus, cells have mechanisms for tightly controlling the turnover rates of their actin networks both spatially as well as temporally. This is achieved through the concerted actions of multiple, highly conserved actin disassembly-promoting factors, including: Actin depolymerizing factor (ADF)/Cofilin, Coronin, AIP1, Srv2/CAP, and Twinfilin [1–5].

ADF/Cofilin and Twinfilin are members of the ADF-homology (ADF-H) domain family of proteins, which are conserved across distant species of animals and fungi. This family also includes actin-binding protein 1 (Abp1)/drebrin, coactosin, and glia maturation factor (GMF). Each member of the larger ADF-H family has a single ADF-H domain, with the exception of Twinfilin, which contains two. Interestingly, each ADF-H family member performs mechanistically distinct functions in regulating the actin cytoskeleton [2]. ADF/Cofilin proteins bind F-actin and induce severing and depolymerization; in addition, they bind and regulate G-actin recycling [6–12]. Abp1 and Coactosin associate specifically with F-actin and influence actin organization in vivo, yet have no known effects on actin filament dynamics in vitro. GMF binds with high affinity to the actin-related protein (Arp) 2/3 complex, rather than actin, and catalyzes actin filament debranching to promote network remodeling and turnover [13–17].

In comparison with other ADF-H family members, Twinfilin has a unique molecular architecture, consisting of two ADF-H domains separated by a short linker region and followed by a short C-terminal tail sequence [18]. Twinfilin was initially characterized as an actin monomer sequestering protein due to its high affinity for ADP-G-actin [18–20]. Subsequently, mouse Twinfilin was shown to associate with the barbed ends and/or sides of actin filaments [21,22]. Twinfilin's function in regulating actin disassembly became clear when yeast Twinfilin was shown to bind F-actin sides and barbed ends, and to catalyze barbed end depolymerization of actin filaments by ~3-fold and, in conjunction with Srv2/CAP (cyclase associated protein), catalyze pointed end depolymerization by ~ 17-fold [23]. What has remained unclear is whether these depolymerization activities of yeast Twinfilin extend to homologs of Twinfilin in other species.

While model organisms such as *Saccharomyces cerevisiae* and *Drosophila melanogaster* have a single Twinfilin gene, mammals have two: Twinfilin-1 and Twinfilin-2 [24]. Alternative splicing of Twinfilin-2 gives rise to two isoforms, Twf2a and Twf2b, which differ minimally in only their N-termini [25]. Thus, mammals express three Twinfilin isoforms in total: Twf1, Twf2a, and Twf2b. Twf1 is found in most cell and tissues types in both developing and adult animals. Twf2a is expressed primarily in adult animals, where it is ubiquitous, but typically found at lower levels compared to Twf1 [26,27]. Twf2b is expressed primarily in cardiac and skeletal muscle. In animal cells, a role for Twinfilin proteins in regulating barbed end dynamics is suggested by their localization to the tips of filopodia, stereocilia, and *Drosophila* bristles [20,28,29]. Moreover, Twinfilin binds directly to Capping Protein, in both yeast and mammalian cells, which further suggests its involvement in barbed end regulation [30,31]. Mammalian Twinfilin isoforms have been shown to be important for regulating cell migration, stereocilia formation, cancer progression, platelet activation, and cardiomyocyte function [28,29,32–36], and there appears to be genetic redundancy between mTwf1 and mTwf2a in vivo [27].

Previous biochemical studies have shown that mouse Twf1, Twf2a, and Twf2b bind with high affinity to ADP-actin monomers and with lower affinity to F-actin, similar to yeast and *Drosophila* Twinfilin [25,30,37,38]. Further, all three isoforms block the elongation of actin filaments in a concentration-dependent manner, suggesting that they cap barbed ends [21,22,25]. As mentioned above, however, it has remained an open question whether the depolymerization activities observed for yeast Twinfilin are conserved in mouse Twinfilin isoforms.

Here we address this question using TIRF microscopy to define the in vitro effects of mouse Twf1, Twf2a, and Twf2b isoforms on barbed and pointed end depolymerization, both in the presence and absence of Srv2/CAP. Our data show that the barbed end, but not pointed end depolymerization activities are conserved in all three mouse Twinfilin isoforms. Further, we dissect requirements for the yeast-specific effects on pointed end depolymerization, and demonstrate that they stem from the C-terminal ADF-H domain, and that these activities can be conferred to mouse Twinfilin by only exchanging this one domain. These results have important implications for mouse Twinfilin in vivo functions, and for how different ADF-H family members contribute to the disassembly of actin networks.

RESULTS

Mouse Twf1, Twf2a, Twf2b catalyze actin barbed end depolymerization.

The three mouse Twinfilin isoforms each share ~20% sequence identity to yeast Twinfilin (Fig. 1A; sequence alignment in Fig. S1). We began by asking whether any of the mouse Twinfilin isoforms are capable of catalyzing barbed and/or pointed end actin filament depolymerization in the presence and absence of the N-terminal half of mouse Srv2/CAP (N-CAP1). Each of the mouse Twinfilin isoforms (mTwf1, mTwf2a, and mTwf2b) was purified as a GST-fusion protein in *E. coli*, and the tag proteolytically removed. TIRF microscopy assays were used to directly observe the depolymerization of individual actin filaments in real time. Our previous work on yeast Twinfilin showed that its effects on depolymerization were specific to aged (ADP) actin, as it failed to catalyze depolymerization of filaments comprised of ADP+P_i actin (generated by adding an excess of free P_i to the reaction) [23]. Therefore, we used preformed filaments to test the effects of mouse Twinfilin isoforms. Filaments were polymerized to a suitable length for depolymerization assays (>10 μm) and sparsely tethered by incorporation of a low percentage of biotin-actin. Then, the chamber was washed out, and proteins of interest (in the absence of actin) were flowed in. Barbed ends were identified by their faster polymerization kinetics before flow-in, enabling us to quantify depolymerization rates at the barbed and pointed ends of the filament separately (Fig. 1B). In control reactions, filaments depolymerized at rates of 1.45 subunits s^{-1} at barbed end (Fig. 1C), and 0.49 subunits s^{-1} at pointed ends (Fig. 1D), similar to previously reported rates [23,39]. Addition of 1 μM mTwf1, mTwf2a, and mTwf2b each increased the rate of barbed end depolymerization by ~2–3 fold, similar to the ~3-fold increase for yeast Twinfilin (Fig. 1C; Table 1; Movie S1). The further addition of 1 μM N-CAP1 enhanced rates of barbed end depolymerization for mTwf2a and mTwf2b, but not mTwfl. Thus, N-CAP1's ability to synergize with Twinfilin in promoting actin filament depolymerization is isoform-specific.

As extra assurance that the actin filaments in our assays above had been aged properly, we compared rates of depolymerization induced by Twinfilin in the first versus second halves of the reactions (15 min observation window), and no statistical difference was observed (Fig. S2A). Additionally, we measured the depolymerization rates of filaments aged for an extra 10 min before flowing in mTwf1, with or without N-CAP1, and found that prolonged aging of filaments did not alter the rates of depolymerization (Fig. S2B).

Analysis of pointed end depolymerization rates revealed striking differences between the effects of yeast Twinfilin and mouse Twinfilin isoforms. Whereas yeast Twinfilin combined with N-Srv2 induced more than a 10-fold increase in the rate of pointed end depolymerization (Table 1), the combination of mouse Twinfilin isoforms and N-CAP1 induced only a modest (~2-fold) increase (Fig. 1D; Table 1). Interestingly, in the absence of Srv2/CAP, yeast Twinfilin and mouse Twinfilin isoforms each caused a similar (~2-fold) increase in pointed end depolymerization.

Taken together, these results suggest that although Twinfilin's effects on barbed end depolymerization are conserved between yeast and mouse isoforms, its ability to induce

rapid depolymerization at pointed ends (in conjunction with Srv2/CAP) is specific to yeast Twinfilin.

N-CAP1 tunes the barbed end depolymerization effects of mouse Twinfilin

Our results above demonstrate that a fixed, relatively high concentration of mouse Twinfilin (1 μM) is sufficient to accelerate barbed end depolymerization, and further addition of mouse N-CAP1 does not enhance this further. However, our previous single molecule analysis showed that yeast N-Srv2 increases the processivity of Twinfilin molecules on the depolymerizing barbed end [23], suggesting that Srv2/CAP may be capable of lowering the effective concentration of Twinfilin required for accelerating barbed end depolymerization. To test this possibility, we measured barbed end depolymerization rates in the presence of a low concentration of mTwf1 (50 nM) and increasing concentrations of N-CAP1 (0.25–5 μM). As expected, 50 nM mTwf1 alone showed no significant effect on barbed end depolymerization rate. Similarly, even a high concentration of N-CAP1 (5 μM) alone had no effect (Fig. 2A). However, 50 nM mTwf1 combined with increasing concentrations of N-CAP1 led to concentration-dependent accelerated barbed end depolymerization (Fig. 2A). These results strongly suggest that mouse Twinfilin and mouse N-CAP1 function in concert to promote barbed end depolymerization.

Rapid pointed end depolymerization requires yeast Twinfilin in combination with either yeast or mouse Srv2/CAP

In principle, the observed species-specific effects of yeast Twinfilin and N-Srv2 on pointed end depolymerization could be due to unique properties of yeast Twinfilin and/or yeast N-Srv2. To address this, we compared rates of barbed and pointed end depolymerization in reactions containing 1 μM yeast or mouse Twinfilin combined with 1 μM yeast or mouse N-Srv2/N-CAP1. N-Srv2 and N-CAP1 alone each had no effect on the rate of depolymerization at barbed ends, as expected. Further, the rate of barbed end depolymerization induced by yeast Twinfilin or mTwf1 was not enhanced by N-Srv2 or N-CAP1 (Fig. 3A). However, N-Srv2 and N-CAP1 were both capable of synergizing with yeast Twinfilin to induce rapid pointed end depolymerization (Fig. 3B), demonstrating that the ability to enhance pointed end depolymerization is conserved between distant Srv2/CAP homologs. In contrast, N-Srv2 and N-CAP1 were unable to synergize with mTwf1 in inducing rapid pointed end depolymerization. Thus, the properties of yeast Twinfilin appear to be distinct from those of mouse Twinfilin, somehow enabling only yeast Twinfilin to work with Srv2/CAP homologs in catalyzing rapid pointed end depolymerization.

Twinfilin chimeras reveal domain requirements for yeast-specific effects on pointed end depolymerization

The results above led us to consider whether the unique pointed end depolymerization effects of yeast Twinfilin are attributed to a specific domain. To address this, we generated a number of chimeras, exchanging different domains between yeast and mouse Twinfilin (Fig. 4A). We then compared the effects of the chimeras on barbed and pointed end depolymerization in TIRF microscopy assays, both in the absence and presence of N-CAP1 (Fig. 4B, C; Table 1). Additionally, the effects of each chimera on pointed end

depolymerization were confirmed in bulk assays using actin filaments capped at their barbed ends by Capping Protein (CapZ) (Fig. 4D, E).

Analysis of pointed end depolymerization rates revealed that introducing the yeast C-terminal ADF-H domain into mouse Twinfilin (construct C3) was sufficient to confer rapid pointed end depolymerization in the presence of N-CAP1 (Fig. 4C). In contrast, swapping the C-terminal 'tail' regions between yeast and mouse Twinfilin (constructs C1 and C4) did not alter their respective effects on depolymerization, and nor did replacing the mouse Twinfilin N-terminal ADF-H domain with that of yeast Twinfilin (construct C2). Thus, the C-terminal ADF-H domain appears to have a central role in specifying pointed end depolymerization effects. It was previously shown that the ability of yeast Twinfilin to induce rapid pointed end depolymerization requires both of its ADF-H domains and the C-terminal tail region, and that none of these domains alone was sufficient for this activity. In light of these observations, the C-terminal ADF-H domain of mouse Twinfilin appears to have diverged from that of yeast Twinfilin, and specifies the key differences in their activities.

Interestingly, our chimera analysis above also revealed that there is a distinct set of requirements for Twinfilin activity in accelerating barbed end depolymerization (Fig. 4B; Table 1). For instance, constructs C1 and C4 were compromised for accelerating barbed end depolymerization, both in the presence or absence of N-CAP1. Thus, the C-terminal tails of yeast and mouse Twinfilin appear to be incompatible with the other domains in catalyzing barbed end depolymerization, and must be matched in a species-specific manner with the remaining portions of Twinfilin. Similarly, constructs exchanging the N- and C-terminal ADF-H domains (C2 and C3, respectively) were compromised in barbed end depolymerization, although C2 had partial activity. Together, these observations reveal that the barbed end effects of yeast and mouse Twinfilin are disrupted by all domain exchanges tested, suggesting that these activities are highly dependent on intra-species compatibility among domains. Importantly, some of the same chimeras that were incapable of catalyzing barbed end depolymerization, with or without N-CAP1, were fully capable of inducing rapid pointed end depolymerization with N-CAP1, highlighting the key differences in molecular requirements for the two activities.

Tropomyosin blocks F-actin severing by ADF/Cofilin but not depolymerization by Twinfilin and N-Srv2/CAP

Finally, we considered how the depolymerization effects of Twinfilin and Srv2/CAP are affected by Tropomyosin decoration of actin filaments. In mammalian cells, it has been proposed that most actin networks are decorated by one or more isoforms of Tropomyosin, which endow networks with different functional properties [40]. More specifically, Tropomyosins have been shown to competitively block the associations of other actin-binding proteins with actin filaments, and to activate specific myosins. However, a key question that has remained open is how Tropomyosin decoration affects the activities of actin disassembly factors. Previous work has shown that several different Tropomyosin isoforms can block ADF/Cofilin interactions with and disassembly of actin filaments [41–

43]. However, the effects of Tropomyosin on Twinfilin-based disassembly have not yet been examined.

To address this question, we initially focused on the yeast system, given that yeast Twinfilin and Srv2/CAP robustly depolymerize both ends of the filament. Further, *S. cerevisiae* express only two isoforms of Tropomyosin, Tpm1 and Tpm2, with one of them (Tpm1) being much more abundant and playing the dominant role in actin cable formation and polarized cell growth [44,45]. Therefore, we asked how Tpm1 decoration of actin filaments affects depolymerization induced by Twinfilin and Srv2, and as a control, severing by yeast ADF/Cofilin (Cof1). Our results show that Tpm1 had little effect on depolymerization at either end of the filament induced by Twinfilin and N-Srv2 (Fig 5. A, B, D), yet inhibited Cof1-mediated severing (Fig. 5C). Thus, Tpm1 decoration protects sides of filaments from Cof1 effects, while leaving filament ends vulnerable to depolymerization by Twinfilin and Srv2. In addition, we tested the effects of a mammalian Tropomyosin isoform (Tpm1.6) on barbed and pointed end depolymerization induced by mTwf1 +/− N-CAP1, and as a control, its effects on filament severing by human Cofilin-1 (hCof1). We observed that Tpm1.6 strongly protects filaments from severing by hCof1, but not depolymerization by mTwf1, either in the presence or absence of N-CAP1 (Fig. 5E-G). Together, these data suggest that the ability to depolymerize Tropomyosin decorated filaments is a conserved function in the Twinfilin family, and points to Twinfilin's potential in vivo role in depolymerizing actin networks decorated by Tropomyosins.

DISCUSSION

In this study, we set out to define the activities of mouse Twinfilin isoforms in catalyzing depolymerization at the barbed and/or pointed ends of actin filaments, and thus learn whether the activities reported earlier for yeast Twinfilin are conserved in mammals. Our results show that each of the three mouse Twinfilin isoforms (mTwf1, mTwf2a, mTwf2b) accelerates barbed end depolymerization by ~2–5-fold, indicating that this is a conserved function of Twinfilin. On the other hand, none of the mouse Twinfilin isoforms induced rapid pointed end depolymerization in conjunction with Srv2/CAP, in striking contrast to yeast Twinfilin (Fig. 1 and Table 1). Thus, there appear to be important species-specific differences in the functions of Twinfilin. Our results also show that a low concentration of Twinfilin, incapable of accelerating depolymerization on its own, becomes sufficient to drive barbed end depolymerization in the presence of the N-terminal half of Srv2/CAP. These results strengthen the view that Srv2/CAP and Twinfilin work in concert to depolymerize barbed ends, and indicate that their joint function at the barbed end is conserved between yeast and mammals.

In addition, we observed strong cross-species compatibility of Srv2/CAP working together with Twinfilin. At the barbed end, either yeast or mouse Srv2/CAP could work with either yeast or mouse Twinfilin to accelerate depolymerization. However, at the pointed end, yeast and mouse Srv2/CAP could work only with yeast Twinfilin (and not mouse Twinfilin) to drive rapid depolymerization. This cross-species compatibility suggests that the structure and function of Srv2/CAP has been maintained across evolution. Consistent with this model, the N-terminal halves of yeast and mouse Srv2/CAP oligomerize into similar, ordered

hexamers with six-fold symmetry, in which the N-terminal helical-folded domains (HFDs) are displayed as 'blades' in a radial configuration [46,47]. Further, the same conserved surfaces on the HFDs of yeast and mouse Srv2/CAP are required for their effects in enhancing ADF/Cofilin and Twinfilin activities [23,46,47]. The molecular architecture of Srv2/CAP may also help explain how it enhances Twinfilin activity at the barbed end. Single molecule studies showed that yeast Twinfilin processively associates with depolymerizing barbed ends of filaments, and that Srv2/CAP enhances Twinfilin processivity [23]. Thus, Srv2/CAP hexamers may cluster Twinfilin molecules at the barbed end and/or provide additional actin-binding sites, via the F-actin binding HFD domains [47], to increase Twinfilin processivity and drive depolymerization. This may explain how Srv2/CAP lowers the concentration of Twinfilin required to catalyze barbed end depolymerization. Resolving this mechanism further, and the potentially-related mechanism of the N-terminal half of Srv2/CAP enhancing ADF/Cofilin-mediated severing, will likely require high resolution structural analysis of Srv2/CAP hexamers and ADF-H proteins bound to F-actin.

Our finding that mouse Twinfilin isoforms lack the robust pointed end depolymerization effects of yeast Twinfilin have potentially important implications for understanding how different ADF-H family members are used in different organisms to drive the disassembly of actin structures. One of the initial clues to Twinfilin's in vivo functions was the observation that *twf1Δ* is synthetic lethal with partial loss-of-function *cof1* alleles [18], suggesting a role for Twinfilin in promoting actin disassembly. This was later extended to genetic relationships with other actin disassembly factors [48]1 Subsequent analysis of yeast Twinfilin revealed that it accelerates barbed and pointed end depolymerization in concert with Srv2/CAP [23]. Our results here suggest that only the effects on barbed end depolymerization are conserved in mouse Twinfilins. It is interesting that all three mouse Twinfilin isoforms had similar effects in stimulating depolymerization, which is consistent with previous studies suggesting that all three isoforms can associate with the barbed end [25]. Further, it reinforces the view that there is high mechanistic conservation among the three isoforms, and that differences in their physiological roles may be attributed instead to their unique expression patterns and localization patterns, and possible difference in cellular binding partners.

Using chimeras, we determined that the unique abilities of yeast Twinfilin to catalyze robust pointed end depolymerization stem specifically from its C-terminal ADF-H domain. Further, we showed that introducing this one domain of yeast Twinfilin into mouse Twinfilin was sufficient to confer pointed end depolymerization effects (Fig. 4; Table 1). These observations demonstrate that differences in the C-terminal ADF-H domains of yeast and mouse Twinfilin must account for the activity difference. While a structure is available for the C-terminal ADF-H domain of mouse Twinfilin, there is no structure available for yeast Twinfilin [22,49], precluding a comparison. Thus, we do not yet understand the structural basis for the activity difference. Our data do not rule out the possibility of post-translational modifications of mouse Twinfilin altering the structure and/or increasing the activity of the C-terminal ADF-H domain to drive robust pointed end depolymerization like yeast Twinfilin. Indeed, proteomic studies have identified several sites on mammalian Twinfilins that are phosphorylated, although it is not yet known how these modifications affect Twinfilin activity or in vivo functions [50,51]. Alternatively, robust pointed end

depolymerization may be a capability of yeast Twinfilin that is not maintained evolutionarily, and may instead be catalyzed by other ADF-H family proteins in mammals. Indeed, human ADF (but not human Cofilin-1) was recently shown to accelerate pointed end depolymerization by ~20-fold, similar to the joint effects of yeast Twinfilin and Srv2/CAP [9,10]. Therefore, it is possible that pointed end depolymerization is regulated primarily by ADF/Cofilin in some species and by Twinfilin in others. This further suggests that minor changes in ADF-H domains can lead to major differences in their activities, highlighting the versatility and plasticity of the ADF-H structural module.

Finally, our work suggests that actin filament depolymerization mechanisms may be employed in vivo to tune the turnover rates of particular actin networks without disrupting their ultrastruture. Tropomyosin decoration of actin filaments has long been known to impair ADF/Cofilin severing [41–43], and consistent with these studies, we found that decoration of filaments with Tropomyosins inhibited severing by yeast and mammalian ADF/Cofilin. However, Tropomyosin decoration did little to impede the depolymerization effects of either yeast or mouse Twinfilin and Srv2/CAP. Taken together, these observations suggest that combining Tropomyosin decoration with depolymerization mechanisms may allow cells to tune the turnover rates of long linear actin arrays (e.g., filopodia, microvilli, stereocilia, sarcomeres, stress fibers, and yeast actin cables), which are known to vary greatly, while maintaining the architectures of these arrays which are so critical to their functions.

EXPERIMENTAL PROCEDURES

Plasmids

Plasmids for expressing yeast Twf1 have been described [23]. To generate plasmids for expressing each mouse Twinfilin isoform as a glutathione-S-transferase (GST)-fusion protein in *E. coli*, the ORFs of each isoform were PCR amplified from pHAT2-mTwf1, pHAT2-mTwf2a, and pHAT2-mTwf2b kindly provided by Pekka Lappalainen (Univ. Helsinki) [25], and subcloned into the EcoRI and NotI sites of pGEX-6p-1, yielding pGEX-6p-1-mTwf1, pGEX-6p-1-mTwf2a, and pGEX-6p-1-mTwf2b. To generate plasmids pGEX-6p-1-C1 and pGEX-6p-1-C4, for expressing Twinfilin chimeric polypeptides in which the tail region of yeast or mouse Twf was exchanged, oligos encoding the tail sequences were synthesized (IDT DNA, Skokie, IL), annealed, and subcloned into BglII and NotI sites (mouse Twf tail) or SalI and NotI sites (yeast Twf tail). To generate plasmids pGEX-6p-1-C2 and pGEX-6p-1-C3, for expressing Twinfilin chimeric polypeptides in which the N-or C-terminal ADF-H domains were exchanged between mouse to yeast isoforms, complete inserts were synthesized (Genewiz, South Plainfield, NJ) and subcloned into pGEX-6p-1 as described above. The pHAT2-N-CAP1 plasmid used to express a 6His-fusion of the N-terminal half of mouse CAP1 (N-CAP1, residues 1–217) was kindly provided by Pekka Lappalainen (Univ. Helsinki) [52].The plasmid for expressing a 6His-fusion of the N-terminal half of yeast Srv2/CAP (N-Srv2) has been described [53]. The plasmid for expressing human Cofilin-1 in *E. coli* was a kind gift from Dr. David Kovar (University of Chicago). The plasmid for expressing yeast Tpm1 in *E. coli* has been described [54]. The plasmid for expressing human Tpm1.6 in *E. coli* was a kind gift from

Dr. Peter Gunning (University of New South Wales). All constructs were verified by DNA sequencing.

Protein expression and purification

Rabbit skeletal muscle actin [55], biotinylated actin [56], pyrenyliodoacetamide-labeled actin (pyrene actin) [57] were purified as described previously. Fluorescent rabbit muscle actin, labeled on Cys^{374} with Oregon Green (OG) maleimide (Life Technologies; Carlsbad, CA) was generated as described [39]. *S. cerevisiae* Tropomyosin (Tpm1) carrying a Met-Ala-Ser extension at its N-terminus to mimic the acetylation of its N-terminal Met (active state) was purified from *E. coli* as described [54]. *S. cerevisiae* ADF/Cofilin (Cof1) was expressed and purified in *E. coli* as described [53].

Twinfilin polypeptides were expressed as GST-fusions in *E. coli* strain BL21 (pRARE). Cells were grown to log phase at 37°C, and then expression was induced for 16 h at 18 °C by addition of 0.4 mM isopropyl-β-D-thiogalactopyranoside (IPTG). Cells were collected by centrifugation, washed with 25 ml water, and resuspended in 10 ml of PBS supplemented freshly with 0.5 mM dithiothreitol (DTT), 1 mM phenylmethylsulphonyl fluoride (PMSF), and a standard mixture of protease inhibitors. Cells were incubated with lysozyme (0.5 mg ml^{-1}) on ice for 15 min and then sonicated. The cell lysate was clarified by centrifugation at 12,500*g* for 20 min and incubated at 4°C (rotating) for at least 2 h with 0.5 ml glutathione-agarose beads (Sigma-Aldrich; St. Louis, MO). Beads were washed three times in PBS supplemented with 1M NaCl and then washed two times in PBS. Then Twinfilin was cleaved from GST by incubation with PreScission Protease (GE Healthcare; Marlborough, MA) overnight at 4°C (rotating). Beads were pelleted, and the supernatant was concentrated to 0.3 ml, and then further purified by size-exclusion chromatography on a Superose12 column (GE Healthcare) equilibrated in HEK buffer (20 mM Hepes pH 7.5, 1 mM EDTA, 50 mM KCl, 0.5 mM DTT). Peak fractions were pooled, concentrated, aliquoted, snap-frozen in liquid N_2, and stored at −80°C.

N-CAP1 and N-Srv2 polypeptides were expressed as His6-fusions in *E. coli* strain BL21 (pRARE), and grown and induced as above. Cells were lysed by sonication in lysis buffer: 20 mM phosphate buffer pH 7.4, 300 mM NaCl, 1 mM DTT supplemented with 10 mM imidazole, and a standard mixture of protease inhibitors. Clarified lysates were incubated with Ni_2+-NTA beads (Qiagen, Valencia, CA) for 90 min at 4°C and then transferred to a poly-prep chromatography column (Bio-Rad). The resin was washed with 10 column volumes of lysis buffer supplemented with 50 mM imidazole. Proteins were eluted with 5 column volumes of lysis buffer supplemented with 250 mM imidazole, concentrated, and purified further on a Superose 6 gel filtration column (GE Healthcare) equilibrated in 20 mM Tris pH 8.0, 100 mM NaCl, and 1 mM DTT. Peak fractions were pooled, concentrated, aliquoted, snap-frozen in liquid N_2, and stored at −80°C.

Human Cofilin-1 (hCof1) was expressed in BL21 (DE3) *E. coli* by growing cells to log phase at 37°C in TB medium, then inducing expression using ImM isopropyl beta-D-1-thiogalactopyranoside at 18°C for 16 h. Cells were harvested by centrifugation and pellets were resuspended in 20 mM Tris pH 8.0, 50 mM NaCl, 1 mM DTT, and protease inhibitors. Cells were lysed by sonication, and the lysate was cleared by centrifugation at 30,000 × *g*

for 30 min. The lysate was loaded on a 5 ml HiTrap HP Q column (GE Healthcare Biosciences; Pittsburgh, PA), and the flow-through was harvested and dialyzed against 20 mM Hepes pH 6.8, 25 mM NaCl, and 1 mM DTT. Dialyzed protein was loaded onto a 5 ml HiTrap SP FF column (GE Healthcare Biosciences), and eluted using a linear gradient of NaCl (20–500 mM). Peak fractions were concentrated, dialyzed against 20 mM Tris pH 8.0, 50 mM KCl, and 1 mM DTT, aliquoted, and stored at −80°C.

Human Tpm1.6 was expressed in BL21 (DE3) *E. coli* as above for hCof1. Cells were harvested by centrifugation, and lysed by sonication in 20 mM Tris, pH 7.5, 0.5 M NaCl, 5 mM $MgCl_2$. The lysate was incubated at 80°C for 10 min, then cooled for 10 min at −20°C, and precleared by centrifugation at 30,000 × *g* for 20 min. The supernatant was isoelectrically precipitated by dropwise addition of 0.3 M HCl to pH 4.7, centrifuged at 5,000 rpm for 15 min at 4°C, after which the pellet was resuspended in 100 mM Tris, pH 7.5, 0.5 M NaCl, 5 mM $MgCl_2$, 1 mM DTT. This precipitation step was repeated once, and the resuspended pellet was dialyzed against 20 mM Hepes, pH 6.8, 50 mM NaCl, 0.5 mM DTT. Dialyzed protein was applied to a 5 ml HiTrap Q HP column (GE Healthcare Biosciences) and eluted with a linear gradient of NaCl (50 to 600 mM). Peak fractions were concentrated, and purified further on a Superose 6 gel filtration column (GE Healthcare Biosciences, Pittsburgh, PA) equilibrated in 20 mM Tris pH 7.5, 50 mM KCl, 2 mM $MgCl_2$ and 1 mM DTT. Peak fractions were pooled, aliquoted, flash-frozen, and stored at −80°C.

Bulk pyrene F-actin disassembly assays

At time zero, pre-assembled F-actin (2 μM final, 10% pyrene-labelled) was mixed with the indicated proteins or control buffer, along with 3 μM Vitamin-D-Binding Protein (VDBP), also known as human plasma Gc-globulin (Sigma-Aldrich, St. Louis, MO). Fluorescence was monitored for 1000 s at 25°C at 365-nm excitation and 407-nm emission in a fluorescence spectrophotometer (Photon Technology International, Edison, NJ).

Total internal reflection fluorescence (TIRF) microscopy

For all experiments, 24×60 mm coverslips (Fisher Scientific; Pittsburg, PA) were cleaned by successive sonications as follows: 60 min in detergent, 20 min in 1 M KOH, 20 min in 1 M HCl min, and 60 min in ethanol. Coverslips were then washed extensively with ddH_2O and dried in an N2-stream. A solution of 80% ethanol pH 2.0, 2 mg/ml methoxy-poly (ethylene glycol)-silane and 2 μg/ml biotin-poly (ethylene glycol)-silane (Laysan Bio Inc.; Arab, AL) was prepared and layered on the cleaned coverslips (200 μl per coverslip). The coverslips were incubated for 16 h at 70°C. To assemble flow cells, PEG-coated coverslips were rinsed extensively with ddH_2O and dried in an N_2-stream, then attached to a prepared flow chamber (Ibidi; Martinsried, German) with double sided tape (2.5 cm × 2 mm × 120 μm) and five min epoxy resin. Flow cells were prepared immediately before use by sequential incubations as follows: 3 min in HEK-BSA (20 mM Hepes pH 7.5, 1 mM EDTA, 50 mM KCl, 1% BSA), 30 s in Streptavidin (0.1 mg/ml in PBS), a fast rinse in HEK-BSA, and then equilibration in 1X TIRF buffer, pH 7.5 (10 mM imidazole, 50 mM KCl, 1 mM $MgCl_2$, 1 mM EGTA, 0.2 mM ATP, 10 mM DTT, 15 mM glucose, 20 μg/ml catalase, 100 μg/ml glucose oxidase, and 0.5% methylcellulose (4000 cP)). To initiate reactions, actin monomers (10% OG-labeled, 0.5% biotinylated) were diluted to 1 μM in TIRF buffer, and immediately

transferred to a flow chamber. After several minutes, once the actin filaments reached an appropriate length (approximately 10 μm), the reaction mixture was replaced with TIRF buffer lacking actin monomers, with or without Twinfilin polypeptides and/or N-Srv2 or N-CAP1. Time-lapse TIRF microscopy was performed using a Nikon-Ti200 inverted microscope equipped with a 150 mW Ar-Laser (Mellot Griot; Carlsbad, CA), a 60X TIRF-objective with a N.A. of 1.49 (Nikon Instruments Inc.; New York, NY), and an EMCCD camera (Andor Ixon; Belfast, Northern Ireland). During recordings, optimal focus was maintained using the perfect focus system (Nikon Instruments Inc). Images were captured every 5 s. The pixel size corresponded to 0.27 μm.

Filament depolymerization rates were determined by tracing filaments in ImageJ (http://rsbweb.nih.gov/ij) and measuring the change in length of individual filaments for 15– 20 min after flow-in, or until filaments disappeared. Differences in fluorescence intensity along the length of the filament provided fiduciary marks that allowed us to distinguish barbed- and pointed-ends. All results shown are data from at least two independent TIRF experiments.

Supplementary Material

Refer to Web version on PubMed Central for supplementary material.

ACKNOWLEDGEMENTS

We are grateful to Sean Guo, M. Angeles Juanes, Silvia Jansen, Thomas Rands, and Shashank Shekhar for helpful discussions and/or comments on the manuscript, and to Julian Eskin for generating the graphical abstract. We are especially grateful to Silvia Jansen for advice throughout the project and for providing purified Tpm1.6. and human Cofilin-1. This work was supported by a grant from the NUT (R01 GM063691) to B.L.G and by Brandeis NSF MRSEC DMR-1420382.

Abbreviations:

ADF	Actin-Depolymerizing Factor
Twf	Twinfilin
Tpm1	Tropomyosin-1
Srv2/CAP	Suppressor of Ras^{Val2}/Cyclase-Associated Protein
TIRF	Total Internal Reflection Fluorescence

REFERENCES

[1]. Ono S The role of cyclase-associated protein in regulating actin filament dynamics - more than a monomer-sequestration factor. J Cell Sci 2013;126:3249–58. doi:10.1242/jcs.128231. [PubMed: 23908377]

[2]. Poukkula M, Kremneva E, Serlachius M, Lappalainen P. Actin-depolymerizing factor homology domain: a conserved fold performing diverse roles in cytoskeletal dynamics. Cytoskeleton (Hoboken) 2011;68:471–90. doi:10.1002/cm.20530. [PubMed: 21850706]

[3]. Chan KT, Creed SJ, Bear JE. Unraveling the enigma: progress towards understanding the coronin family of actin regulators. Trends Cell Biol 2011;21:481–8. doi:10.1016/j.tcb.2011.04.004. [PubMed: 21632254]

[4]. Ono S Mechanism of depolymerization and severing of actin filaments and its significance in cytoskeletal dynamics. Int Rev Cytol 2007;258:1–82. doi:10.1016/S0074-7696(07)58001-0. [PubMed: 17338919]

[5]. Hild G, Kalmar L, Kardos R, Nyitrai M, Bugyi B. The other side of the coin: functional and structural versatility of ADF/cofilins. Eur J Cell Biol 2014;93:238–51. doi:10.1016/j.ejcb.2013.12.001. [PubMed: 24836399]

[6]. Hayden SM, Miller PS, Brauweiler A, Bamburg JR. Analysis of the interactions of actin depolymerizing factor with G- and F-actin. Biochemistry 1993;32:9994–10004. [PubMed: 8399168]

[7]. Carlier MF, Laurent V, Santolini J, Melki R, Didry D, Xia GX, et al. Actin depolymerizing factor (ADF/cofilin) enhances the rate of filament turnover: implication in actin-based motility. J Cell Biol 1997;136:1307–22. [PubMed: 9087445]

[8]. Hawkins M, Pope B, Maciver SK, Weeds AG. Human actin depolymerizing factor mediates a pH-sensitive destruction of actin filaments. Biochemistry 1993;32:9985–93. [PubMed: 8399167]

[9]. Shekhar S, Carlier M-F. Enhanced Depolymerization of Actin Filaments by ADF/Cofilin and Monomer Funneling by Capping Protein Cooperate to Accelerate Barbed-End Growth. Curr Biol 2017;27:1990–1998.e5. doi:10.1016/j.cub.2017.05.036. [PubMed: 28625780]

[10]. Wioland H, Guichard B, Senju Y, Myram S, Lappalainen P, Jégou A, et al. Adf/cofilin accelerates actin dynamics by severing filaments and promoting their depolymerization at both ends. Curr Biol 2017;27:1956–1967.e7. doi:10.1016/j.cub.2017.05.048. [PubMed: 28625781]

[11]. Nishida E Opposite effects of cofilin and profilin from porcine brain on rate of exchange of actin-bound adenosine 5'-triphosphate. Biochemistry 1985;24:1160–4. [PubMed: 4096896]

[12]. Nishida E, Maekawa S, Sakai H. Cofilin, a protein in porcine brain that binds to actin filaments and inhibits their interactions with myosin and tropomyosin. Biochemistry 1984;23:5307–13. [PubMed: 6509022]

[13]. Gandhi M, Smith BA, Bovellan M, Paavilainen V, Daugherty-Clarke K, Gelles J, et al. GMF is a cofilin homolog that binds Arp2/3 complex to stimulate filament debranching and inhibit actin nucléation. Curr Biol 2010;20:861–7. doi:10.1016/j.cub.2010.03.026. [PubMed: 20362448]

[14]. Ydenberg CA, Padrick SB, Sweeney MO, Gandhi M, Sokolova O, Goode BL. GMF severs actin-Arp2/3 complex branch junctions by a cofilin-like mechanism. Curr Biol 2013;23:1037–45. doi:10.1016/j.cub.2013.04.058. [PubMed: 23727094]

[15]. Poukkula M, Hakala M, Pentinmikko N, Sweeney MO, Jansen S, Mattila J, et al. GMF promotes leading-edge dynamics and collective cell migration in vivo. Curr Biol 2014;24:2533–40. doi:10.1016/j.cub.2014.08.066. [PubMed: 25308079]

[16]. Luan Q, Nolen BJ. Structural basis for regulation of Arp2/3 complex by GMF. Nat Struct Mol Biol 2013;20:1062–8. doi:10.1038/nsmb.2628. [PubMed: 23893131]

[17]. Haynes EM, Asokan SB, King SJ, Johnson HE, Haugh JM, Bear JE. GMFß controls branched actin content and lamellipodial retraction in fibroblasts. J Cell Biol 2015;209:803–12. doi:10.1083/jcb.201501094. [PubMed: 26101216]

[18]. Goode BL, Drubin DG, Lappalainen P. Regulation of the cortical actin cytoskeleton in budding yeast by twinfilin, a ubiquitous actin monomer-sequestering protein. J Cell Biol 1998;142:723–33. [PubMed: 9700161]

[19]. Vartiainen M, Ojala PJ, Auvinen P, Peränen J, Lappalainen P. Mouse A6/twinfilin is an actin monomer-binding protein that localizes to the regions of rapid actin dynamics. Mol Cell Biol 2000;20:1772–83. [PubMed: 10669753]

[20]. Wahlström G, Vartiainen M, Yamamoto L, Mattila PK, Lappalainen P, Heino TI. Twinfilin is required for actin-dependent developmental processes in Drosophila. J Cell Biol 2001;155:787–96. doi:10.1083/jcb.200108022. [PubMed: 11724820]

[21]. Helfer E, Nevalainen EM, Naumanen P, Romero S, Didry D, Pantaloni D, et al. Mammalian twinfilin sequesters ADP-G-actin and caps filament barbed ends: implications in motility. EMBO J 2006;25:1184–95. doi:10.1038/sj.emboj.7601019. [PubMed: 16511569]

[22]. Paavilainen VO, Hellman M, Helfer E, Bovellan M, Annila A, Carlier M-F, et al. Structural basis and evolutionary origin of actin filament capping by twinfilin. Proc Natl Acad Sci USA 2007;104:3113–8. doi:10.1073/pnas.0608725104. [PubMed: 17360616]

[23]. Johnston AB, Collins A, Goode BL. High-speed depolymerization at actin filament ends jointly catalysed by Twinfilin and Srv2/CAP. Nat Cell Biol 2015;17:1504–11. doi: 10.1038/ncb3252. [PubMed: 26458246]

[24]. Palmgren S, Vartiainen M, Lappalainen P. Twinfilin, a molecular mailman for actin monomers. J Cell Sci 2002;115:881–6. [PubMed: 11870207]

[25]. Nevalainen EM, Skwarek-Maruszewska A, Braun A, Moser M, Lappalainen P. Two biochemically distinct and tissue-specific twinfilin isoforms are generated from the mouse Twf2 gene by alternative promoter usage. Biochem J 2009;417:593–600. doi: 10.1042/BJ20080608. [PubMed: 18837697]

[26]. Vartiainen MK, Sarkkinen EM, Matilainen T, Salminen M, Lappalainen P. Mammals have two twinfilin isoforms whose subcellular localizations and tissue distributions are differentially regulated. J Biol Chem 2003;278:34347–55. doi:10.1074/jbc.M303642200. [PubMed: 12807912]

[27]. Nevalainen EM, Braun A, Vartiainen MK, Serlachius M, Andersson LC, Moser M, et al. Twinfilin-2a is dispensable for mouse development. PLoS One 201l;6:e22894. doi:10.1371/journal.pone.0022894. [PubMed: 21876732]

[28]. Peng AW, Belyantseva IA, Hsu PD, Friedman TB, Heller S. Twinfilin 2 regulates actin filament lengths in cochlear stereocilia. J Neurosci 2009;29:15083–8. doi:10.1523/JNEUROSCI.2782-09.2009. [PubMed: 19955359]

[29]. Rzadzinska AK, Nevalainen EM, Prosser HM, Lappalainen P, Steel KP. MyosinVIIa interacts with Twinfilin-2 at the tips of mechanosensory stereocilia in the inner ear. PLoS One 2009;4:e7097. doi:10.1371/journal.pone.0007097. [PubMed: 19774077]

[30]. Palmgren S, Ojala PJ, Wear MA, Cooper JA, Lappalainen P. Interactions with PIP2, ADP-actin monomers, and capping protein regulate the activity and localization of yeast twinfilin. J Cell Biol 2001;155:251–60. doi:10.1083/jcb.200106157. [PubMed: 11604420]

[31]. Falck S, Paavilainen VO, Wear MA, Grossmann JG, Cooper JA, Lappalainen P. Biological role and structural mechanism of twinfilin-capping protein interaction. EMBO J 2004;23:3010–9. doi: 10.1038/sj.emboj.7600310. [PubMed: 15282541]

[32]. Bockhorn J, Dalton R, Nwachukwu C, Huang S, Prat A, Yee K, et al. MicroRNA-30c inhibits human breast tumour chemotherapy resistance by regulating TWF1 and IL-11. Nat Commun 2013;4:1393. doi:10.1038/ncomms2393. [PubMed: 23340433]

[33]. Meacham CE, Ho EE, Dubrovsky E, Gertler FB, Hemann MT. In vivo RNAi screening identifies regulators of actin dynamics as key determinants of lymphoma progression. Nat Genet 2009;41:1133–7. doi:10.1038/ng.451. [PubMed: 19783987]

[34]. Stritt S, Beck S, Becker IC, Vögtle T, Hakala M, Heinze KG, et al. Twinfilin 2a is a regulator of platelet reactivity and turnover in mice. Blood 2017;130:1746–56. doi:10.1182/blood-2017-02-770768. [PubMed: 28743718]

[35]. Li Q, Song X-W, Zou J, Wang G-K, Kremneva E, Li X-Q, et al. Attenuation of microRNA-1 derepresses the cytoskeleton regulatory protein twinfilin-1 to provoke cardiac hypertrophy. J Cell Sci 2010;123:2444–52. doi:10.1242/jcs.067165. [PubMed: 20571053]

[36]. Wang D, Zhang L, Zhao G, Wahlström G, Heino TI, Chen J, et al. Drosophila twinfilin is required for cell migration and synaptic endocytosis. J Cell Sci 2010;123:1546–56. doi:10.1242/jcs.060251. [PubMed: 20410372]

[37]. Ojala PJ, Paavilainen VO, Vartiainen MK, Tuma R, Weeds AG, Lappalainen P. The two ADF-H domains of twinfilin play functionally distinct roles in interactions with actin monomers. Mol Biol Cell 2002;13:3811–21. doi:10.1091/mbc.E02-03-0157. [PubMed: 12429826]

[38]. Paavilainen VO, Merckel MC, Falck S, Ojala PJ, Pohl E, Wilmanns M, et al. Structural conservation between the actin monomer-binding sites of twinfilin and actin-depolymerizing factor (ADF)/cofilin. J Biol Chem 2002;277:43089–95. doi:10.1074/jbc.M208225200. [PubMed: 12207032]

[39]. Kuhn JR, Pollard TD. Real-time measurements of actin filament polymerization by total internal reflection fluorescence microscopy. Biophys J 2005;88:1387–402. doi:10.1529/biophysj.104.047399. [PubMed: 15556992]

[40]. Gunning PW, Hardeman EC, Lappalainen P, Mulvihill DP. Tropomyosin - master regulator of actin filament function in the cytoskeleton. J Cell Sci 2015;128:2965–74. doi:10.1242/jcs.172502. [PubMed: 26240174]

[41]. Gateva G, Kremneva E, Reindl T, Kotila T, Kogan K, Gressin L, et al. Tropomyosin isoforms specify functionally distinct actin filament populations in vitro. Curr Biol 2017;27:705–13. doi:10.1016/j.cub.2017.01.018. [PubMed: 28216317]

[42]. Ono S, Ono K. Tropomyosin inhibits ADF/cofilin-dependent actin filament dynamics. J Cell Biol 2002;156:1065–76. doi:10.1083/jcb.200110013. [PubMed: 11901171]

[43]. Bryce NS, Schevzov G, Ferguson V, Percival JM, Lin JJ-C, Matsumura F, et al. Specification of actin filament function and molecular composition by tropomyosin isoforms. Mol Biol Cell 2003;14:1002–16. doi:10.1091/mbc.E02-04-0244. [PubMed: 12631719]

[44]. Drees B, Brown C, Barrell BG, Bretscher A. Tropomyosin is essential in yeast, yet the TPM1 and TPM2 products perform distinct functions. J Cell Biol 1995;128:383–92. [PubMed: 7844152]

[45]. Liu HP, Bretscher A. Disruption of the single tropomyosin gene in yeast results in the disappearance of actin cables from the cytoskeleton. Cell 1989;57:233–42. [PubMed: 2649250]

[46]. Chaudhry F, Breitsprecher D, Little K, Sharov G, Sokolova O, Goode BL. Srv2/cyclase-associated protein forms hexameric shurikens that directly catalyze actin filament severing by cofilin. Mol Biol Cell 2013;24:31–41. doi:10.1091/mbc.E12-08-0589. [PubMed: 23135996]

[47]. Jansen S, Collins A, Golden L, Sokolova O, Goode BL. Structure and mechanism of mouse cyclase-associated protein (CAP1) in regulating actin dynamics. J Biol Chem 2014;289:30732–42. doi:10.1074/jbc.M114.601765. [PubMed: 25228691]

[48]. Ydenberg CA, Johnston A, Weinstein J, Bellavance D, Jansen S, Goode BL. Combinatorial genetic analysis of a network of actin disassembly-promoting factors. Cytoskeleton (Hoboken) 2015;72:349–61. doi:10.1002/cm.21231. [PubMed: 26147656]

[49]. Goroncy AK, Koshiba S, Tochio N, Tomizawa T, Sato M, Inoue M, et al. NMR solution structures of actin depolymerizing factor homology domains. Protein Sci 2009;18:2384–92. doi:10.1002/pro.248. [PubMed: 19768801]

[50]. Mertins P, Yang F, Liu T, Mani DR, Petyuk VA, Gillette MA, et al. Ischemia in tumors induces early and sustained phosphorylation changes in stress kinase pathways but does not affect global protein levels. Mol Cell Proteomics 2014;13:1690–704. doi:10.1074/mcp.M113.036392. [PubMed: 24719451]

[51]. Sharma K, D'Souza RCJ, Tyanova S, Schaab C, Wiśniewski JR, Cox J, et al. Ultradeep human phosphoproteome reveals a distinct regulatory nature of Tyr and Ser/Thr-based signaling. Cell Rep 2014;8:1583–94. doi:10.1016/j.celrep.2014.07.036. [PubMed: 25159151]

[52]. Makkonen M, Bertling E, Chebotareva NA, Baum J, Lappalainen P. Mammalian and malaria parasite cyclase-associated proteins catalyze nucleotide exchange on G-actin through a conserved mechanism. J Biol Chem 2013;288:984–94. doi:10.1074/jbc.M112.435719. [PubMed: 23184938]

[53]. Quintero-Monzon O, Jonasson EM, Bertling E, Talarico L, Chaudhry F, Sihvo M, et al. Reconstitution and dissection of the 600-kDa Srv2/CAP complex: roles for oligomerization and cofilin-actin binding in driving actin turnover. J Biol Chem 2009;284:10923–34. doi:10.1074/jbc.M808760200. [PubMed: 19201756]

[54]. Alioto SL, Garabedian MV, Bellavance DR, Goode BL. Tropomyosin and Profilin Cooperate to Promote Formin-Mediated Actin Nucléation and Drive Yeast Actin Cable Assembly. Curr Biol 2016;26:3230–7. doi:10.1016/j.cub.2016.09.053. [PubMed: 27866892]

[55]. Spudich JA, Watt S. The regulation of rabbit skeletal muscle contraction. I. Biochemical studies of the interaction of the tropomyosin-troponin complex with actin and the proteolytic fragments of myosin. J Biol Chem 1971;246:4866–71. [PubMed: 4254541]

[56]. Breitsprecher D, Jaiswal R, Bombardier JP, Gould CJ, Gelles J, Goode BL. Rocket launcher mechanism of collaborative actin assembly defined by single-molecule imaging. Science (80-) 2012;336:1164–8. doi:10.1126/science.1218062.

[57]. Pollard TD, Cooper JA. Quantitative analysis of the effect of Acanthamoeba profilin on actin filament nucléation and elongation. Biochemistry 1984;23:6631–41. [PubMed: 6543322]

Highlights:

- All three mouse Twinfilin isoforms promote barbed end depolymerization
- Robust pointed end depolymerization is stimulated by yeast but not mouse Twinfilin
- Yeast Twinfilin depolymerizes pointed ends with either yeast or mouse Srv2/CAP
- Yeast Twinfilin pointed end depolymerization depends on its C-terminal ADF-H domain

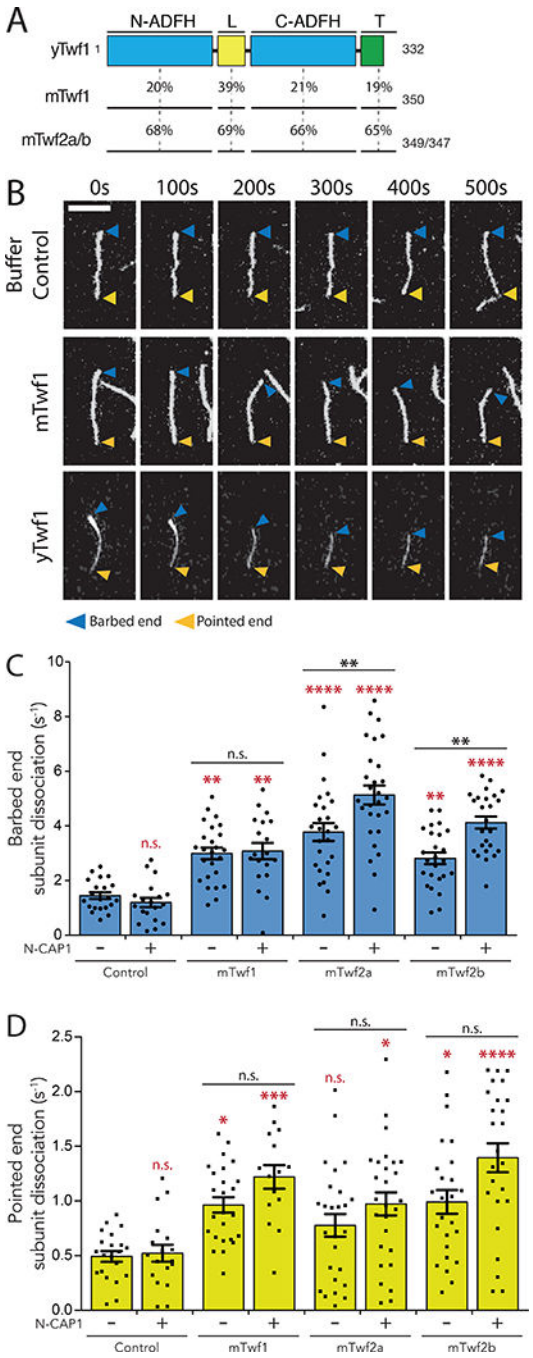

Figure 1. Rates of accelerated actin filament depolymerization by mouse Twinfilin isoforms in the absence or presence of N-CAP1.

(A) Domain organization and amino acid sequence conservation between yeast and mouse Twinfilins: ADF-H, actin depolymerization factor homology domain; L, linker; T, tail. Percentages indicate the protein sequence identity between corresponding domains connected by dotted lines (yTwf1 to mTwf1; mTwf1 to mTwf2a/b). **(B)** Representative time-lapse TIRF microscopy images of tethered actin filaments (10% OG-labeled, 0.5% biotin–actin) depolymerizing in the presence or absence of 1 μM mouse Twinfilin-1 (mTwf1) or 1

μM yeast Twinfilin (yTwf1). Blue arrowheads, barbed ends; yellow arrowheads, pointed ends. Scale bar, 10 μm. **(C)** Rates of barbed end depolymerization (subunits s^{-1}) induced by 1 μM of the indicated mouse Twinfilin isoform, in the absence or presence of 1 μM of the N-terminal half of CAP1 (N-CAP1), measured from TIRF reactions as in (B). Rates for each condition averaged from at least 5 filaments in each of three independent experiments. From left to right: n = 21, 19, 25, 19, 26, 28, 25, and 25 filaments, and mean depolymerization rates of 1.448, 1.196, 2.991, 3.08, 3.773, 5.131, 2.813, and 4.122 subunits s^{-1}. **(D)** Rates of pointed end depolymerization for filaments in the same reactions as in (C). From left to right: n = 21, 18, 25, 15, 26, 27, 25, and 25 filaments, and mean depolymerization rates of 0.493, 0.522, 0.963, 1.219, 0.776, 0.972, 0.991, and 1.395 subunits s^{-1} Error bars, s.e.m. **** $p \leq 0.0001$, *** $p \leq 0.001$, ** $p \leq 0.01$, n.s. $p > 0.05$ by one-way ANOVA with Tukey post hoc test.

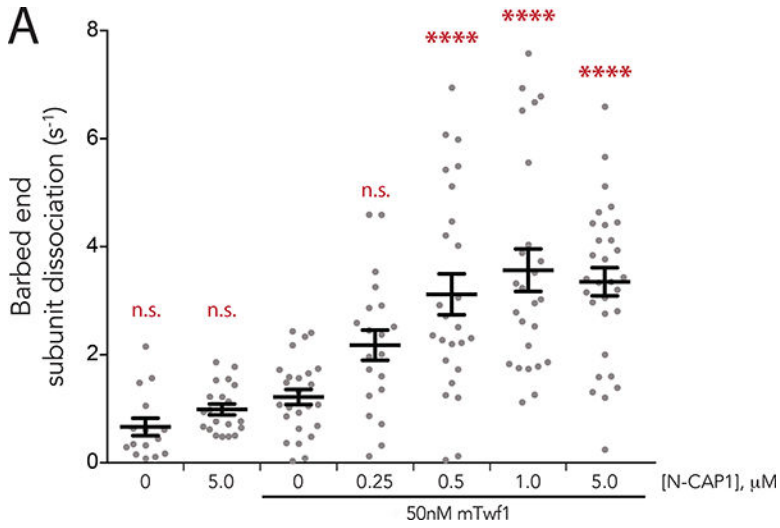

Figure 2. Threshold effects of N-CAP1 in synergizing with mTwf1 to accelerate depolymerization at barbed ends.

(A) Rates of actin filament barbed end depolymerization (subunits s^{-1}) induced by 50 nM mTwf1 in conjunction with increasing concentrations of N-CAP1 (0–5 μM). Rates for each condition were averaged from at least 5 filaments in each of two independent experiments. From left to right: n = 15, 20, 25, 20, 25, 25, and 30 filaments, and mean depolymerization rates of 0.664, 0.987, 1.218, 2.177, 3.117, 3.565, and 3.35 subunits s^{-1}. Error bars, s.e.m. ****$p \leq 0.0001$, n.s. $p > 0.05$ by one-way ANOVA with Tukey post hoc test.

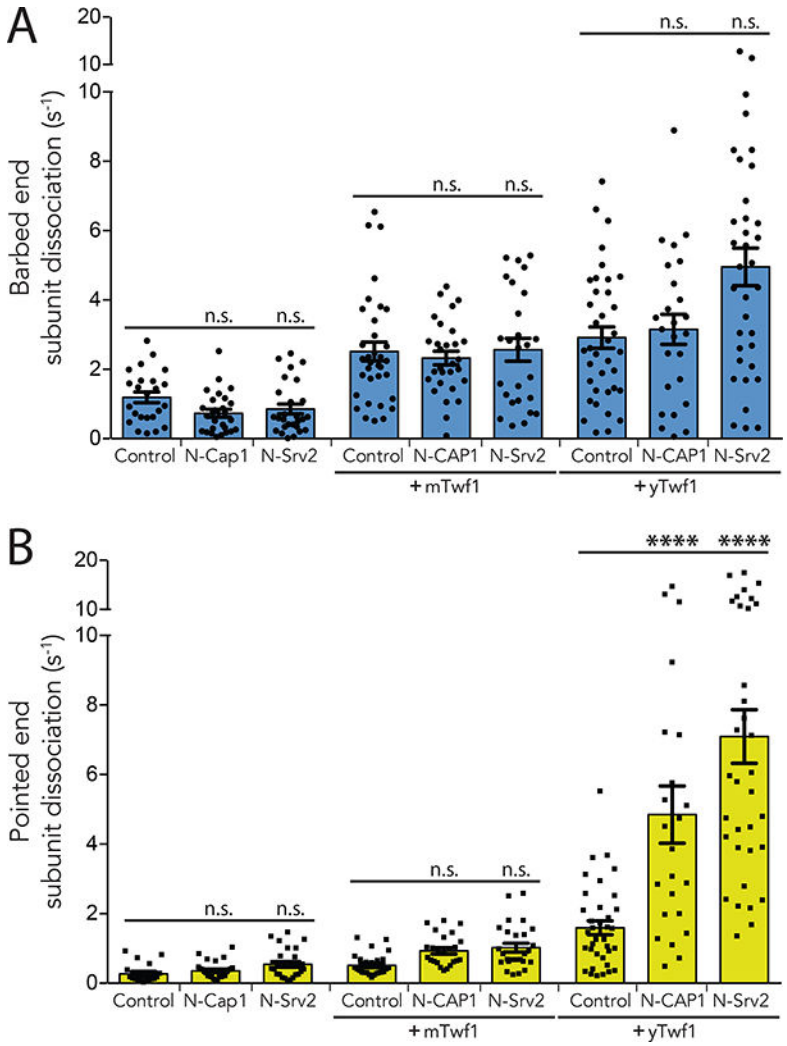

Figure 3. Rates of accelerated actin filament depolymerization induced by mouse and yeast Twinfilins in the absence or presence of mouse or yeast Srv2/CAP.

(A) Comparison of barbed end depolymerization rates (subunits s^{-1}) induced by 1 μM of the indicated Twinfilin protein, in the absence or presence of 1 μM mouse N-CAP1 or yeast N-Srv2. Rates for each condition were averaged from at least 5 filaments in each of three independent experiments. From left to right: n = 24, 27, 27, 34, 29, 26, 37, 25, and 35 filaments, and mean depolymerization rates of 1.191, 0.729, 0.855, 2.512, 2.324, 2.563, 2.913, 3.152, and 4.954 subunits s^{-1}. **(B)** Pointed end depolymerization rates for filaments in the same reactions as in (A). From left to right: n= 17, 24, 27, 25, 24, 26, 36, 23, and 34 filaments, and mean depolymerization rates of 0.268, 0.354, 0.542, 0.514, 0.929, 1.023, 1.593, 4.848, and 7.092 subunits s 1. Error bars, s.e.m. ****$p \leq 0.0001$, n.s. $p > 0.05$ by one-way ANOVA with Tukey post hoc test.

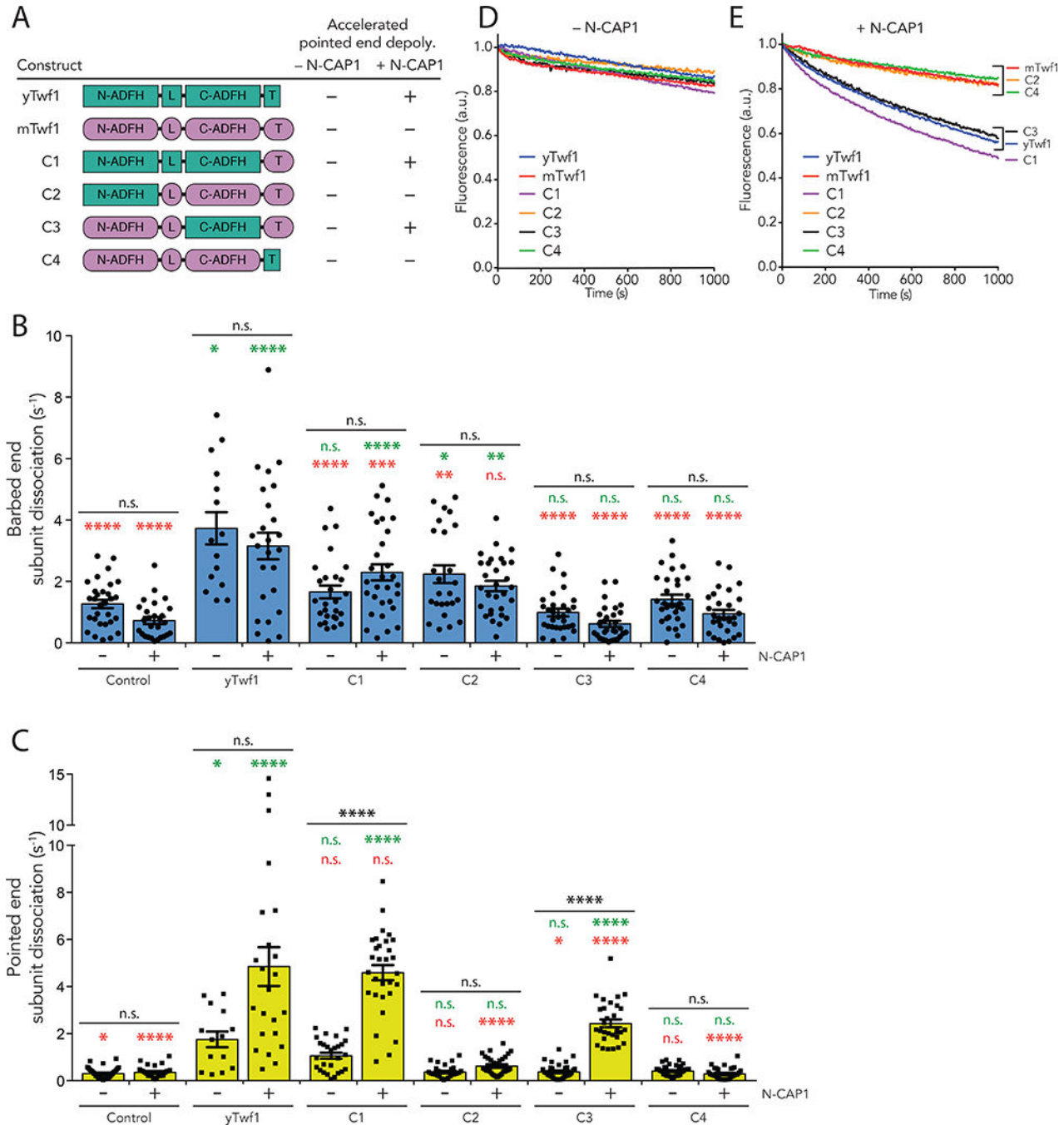

Figure 4. Rates of actin filament depolymerization induced by mouse-yeast Twinfilin chimeras in the absence or presence or mouse N-CAP1.

(A) Schematic of Twinfilin constructs tested and summary of their pointed end activities from TIRF assays in (C). ADF-H, actin depolymerization factor-homology domain; L, linker; T, tail. Domains color-coded by species: yeast (turquoise) and mouse (magenta). **(B)** Rates of barbed end depolymerization (subunits s^{-1}) from TIRF assays in the presence of different Twinfilin constructs (1μM each), with or without 1 μM N-CAP1. Rates for each condition averaged from at least 5 filaments in each of three independent experiments. From

left to right: n = 30, 27, 15, 25, 27, 30, 25, 30, 30, 30, 30, and 30 filaments, and mean depolymerization rates of 1.267, 0.7299, 3.731, 3.152, 1.66, 2.295, 2.237, 1.852, 0.989, 0.619, 1.417, and 0.946 subunits s^{-1}. **(C)** Rates of pointed end depolymerization from filaments in the same TIRF reactions as in (B). From left to right: n = 30, 24, 14, 23, 27, 30, 25, 30, 30, 30, 30, and 29 filaments, and mean depolymerization rates of 0.301, 0.354, 1.756, 4.848, 1.062, 4.59, 0.367, 0.621, 0.376, 2.433, 0.409, and 0.288 subunits s^{-1}. **(D)** Bulk assays showing effects of Twinfilin polypeptides on pointed end depolymerization. Reactions contain 2 μM F-Actin (10% pyrene-labelled), 25 nM Capping Protein (CapZ) to cap barbed ends, and 1 μM of the Twinfilin construct. Disassembly is induced at time zero by the addition of 3 μM vitamin D-binding protein, which sequesters actin monomers. **(E)** Bulk assays as in (D) except with the further addition of 1 μM N-CAP1. Error bars, s.e.m. **** $p \leq 0.0001$, *** $p \leq 0.001$, ** $p \leq 0.01$, * $p \leq 0.05$, n.s. $p > 0.05$ by one-way ANOVA with Tukey post hoc test. Red asterisks, compared to ‘yTwf1’ (+/− N-CAP1). Green asterisks, compared to ‘control’ (+/−N-CAP1).

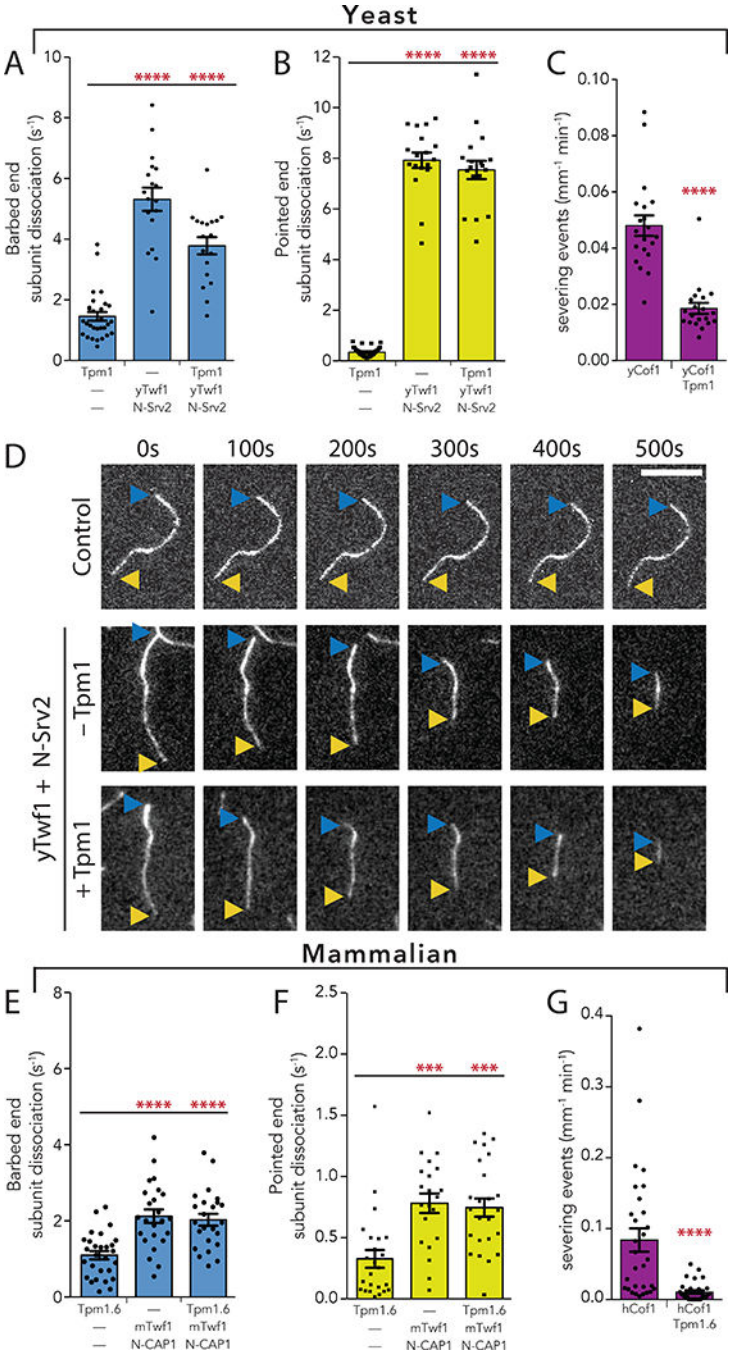

Figure 5. Twinfilin depolymerization effects on Tropomyosin-decorated actin filaments.

Experiments in panels A-D use yeast Twinfilin, Srv2/CAP, ADF/Cofilin, and Tropomyosin, whereas experiments in panels E-G use the mammalian counterparts to these proteins. **(A)** Rates of barbed end depolymerization (subunits s^{-1}) measured in TIRF assays. Actin filaments were first assembled and tethered using 1 μM actin (10% OG-labeled, 0.5% biotin-actin). Then, 1 μM yeast Twinfilin (yTwf1) with or without 1 μM N-Srv2 was flowed in, and depolymerization rates were measured. Where indicated, yeast Tpm1 (2.5 μM) was included both in the initial actin filament assembly and in the subsequent flow in. Rates for each

condition were averaged from at least 5 filaments in each of two independent experiments. From left to right: n = 29, 18, and 18 filaments, and mean depolymerization rates of 1.455, 5.314, and 3.783 subunits s^{-1}. **(B)** Rates of pointed end depolymerization for filaments in the same reactions as in (A). From left to right: n = 29, 18, and 18 filaments, and mean depolymerization rates of 0.341, 7.918, and 7.54 subunits s^{-1}. **(C)** Tpm1 inhibits yeast Cofilin (yCof1)-induced severing of actin filaments. Actin filaments were assembled as above, with or without Tpml, and then 10 nM Cof1 was flowed in, with or without Tpm1, and severing rates (breaks μm^{-1} min^{-1}) were measured. Severing rates for each condition were averaged from at least 10 filaments in each of two independent experiments (n = 20 filaments total). From left to right, mean severing rates are: 0.048 and 0.018 events μm^{-1} min^{-1}. **(D)** Representative time-lapse TIRF microscopy images of tethered actin filaments (10% OG-labeled, 0.5% biotin-actin) depolymerizing in the presence or absence of 1 μM yeast Twinfilin (yTwf1) and 1 μM N-Srv2, in the presence or absence of yeast Tropomyosin (Tpm1). Blue arrowheads, barbed ends; yellow arrowheads, pointed ends. Scale bar, 10 μm. **(E)** Rates of barbed end depolymerization (subunits s^{-1}) measured in TIRF assays in the presence of 1 μM mouse Twinfilin (mTwf1) with or without 1 μM mouse N-CAP1. Where indicated, human Tpm1.6 (2 μM) was included both in the initial actin filament assembly, and in the subsequent flow in. Rates for each condition were averaged from at least 10 filaments in each of two independent experiments. From left to right: n = 28, 24, and 24 filaments, and mean depolymerization rates of 1.10, 2.12, and 2.03 subunits s^{-1}. **(F)** Rates of pointed end depolymerization for filaments in the same reactions as in (D). From left to right: n= 24, 21, and 24 filaments, and mean depolymerization rates of 0.331, 0.782, and 0.747 subunits s^{-1}. **(G)** Tpm1.6 inhibits actin filament severing by human Cofilin (hCof1). Filaments were assembled as above, with or without Tpml.6, and then 150 nM hCof1 was flowed in, with or without Tpm1.6, and severing rates (breaks μm^{-1} min^{-1}) were measured. Severing rates for each condition were averaged from at least 15 filaments in each of two independent experiments (n = 30 filaments total). From left to right, mean severing rates are: 0.084 and 0.010 events μm^{-1} min^{-1}. Error bars, s.e.m. ****$p \leq 0.0001$, *** $p \leq 0.001$, by one-way ANOVA with Tukey post hoc test.

Table 1.

Summary of depolymerization for all Twinfilin constructs

Construct depolymerization rate (subunits $^{-1}$)			
Construct		**Barbed end**	**Pointed End**
Buffer Control	−N-CAP1	1.27 ± 0.14	0.301 ± 0.04
	+ N-CAP1	0.73 ± 0.11	0.354 ± 0.05
yTwfl (WT)	−N-CAP1	3.73 ± 0.52	1.76 ± 0.33
	+ N-CAP1	3.15 ±0.43	4.85 ± 0.82
yTwfl (WT)	−N-Srv2	3.73 ± 0.52	1.76 ± 0.33
	+ N-Srv2	4.95 ± 0.54	7.09 ± 0.76
mTwfl (WT)	−N-CAP1	2.99 ± 0.22	0.963 ± 0.07
	+ N-CAP1	3.08 ± 0.29	1.21 ± 0.11
Twf1-C1	−N-CAP1	1.66 ± 0.21	1.06 ± 0.13
	+ N-CAP1	2.29 ± 0.26	4.59 ± 0.32
Twf1-C2	−N-CAP1	2.24 ± 0.29	0.367 ± 0.05
	+ N-CAP1	1.85 ±0.17	0.622 ± 0.07
Twf1 -C3	−N-CAP1	0.99 ±0.12	0.376 ± 0.06
	+ N-CAP1	0.62 ± 0.09	2.43 ± 0.16
Twf 1-C4	−N-CAP1	1.42 ± 0.15	0.41 ± 0.04
	+ N-CAP1	0.946 ±0.13	0.288 ± 0.05
mTwf2a (WT)	−N-CAP1	3.77 ± 0.33	0.776 ±0.10
	+ N-CAP1	5.13 ± 0.35	0.972 ±0.11
mTwf2b (WT)	−N-CAP1	2.81 ± 0.21	0.991 ±0.11
	+ N-CAP1	4.12 ±0.22	1.395 ±0.13